High-throughput sequencing reveals that microRNA from exosomes as potential pathogenetic factors and biomarkers of moyamoya disease

Da Huang (dah2021@yeah.net)
Peking University Shenzhen Hospital
Hui Qi
Peking University Shenzhen Hospital
Hongchun Yang
Peking University Shenzhen Hospital
Meng chen
Peking University Shenzhen Hospital

Research Article

Keywords: moyamoya disease, exosomes, microRNA, the actin cytoskeleton signalling pathway, plasma, biomarkers

Posted Date: March 10th, 2022

DOI: https://doi.org/10.21203/rs.3.rs-1218259/v1

Abstract

Background: As a progressive cerebrovascular disease, moyamoya disease is a common cause of stroke in children and adults; however, early biomarkers and the pathogenesis of moyamoya disease remain poorly understood.

Objectives: We aimed to diagnose moyamoya disease by identifying noninvasive rapid liquid diagnostic biomarkers using plasma exosomal microRNAs (miRNAs).

Materials and Methods: For the first time, frozen plasma samples from moyamoya disease patients, next-generation high-throughput sequencing technologies, real-time quantitative PCR, gene ontology analysis and Kyoto Encyclopaedia of Genes and Genomes pathway analysis analyses of exosomal miRNA-related target gene functions were used to identify plasma exosomal miRNAs as potential biomarkers of moyamoya disease. The area under the curve of the receiver operating characteristic (ROC) curve was used to evaluate the sensitivity and specificity of biomarkers for predicting events

Results: The target genes of the different expression miRNA showed that they were mainly enriched in axon guidance, regulation of the actin cytoskeleton and the MAPK signalling pathway. Ten miRNAs (miR-1306-5p, miR-196b-5p, miR-19a-3p, miR-22-3p, miR-320b, miR-34a-5p, miR-485-3p, miR-489-3p, miR-501-3p, and miR-487-3p) were found to be associated with the most sensitive and specific pathways for predicting moyamoya disease.

Conclusions: Plasma exosomal miRNAs could be used to construct an accurate predictive model for improving moyamoya disease detection.

1 Introduction

Moyamoya disease is a cerebrovascular disease with unknown aetiology and progressive, occlusive and abnormal collateral vascular networks. However, its pathogenesis is still unknown [1)]. As a rare cerebrovascular disease, moyamoya disease is characterized by bilateral progressive basilar artery stenosis and occlusion and coexisting abnormal reticular vessels. This compensatory collateral circulation network at the bottom of the brain is called moyamoya vessels [2)]. The disease usually involves both hemispheres, although in some patients, arterial stenosis or occlusion occurs only on one side, which is called unilateral moyamoya disease [3)]. A more specific definition of moyamoya disease is idiopathic occlusion of bilateral vessels in the "Willis" arterial ring. The consensus definition involves the most critical features of the disease, namely, the specific location (Willis ring), pathophysiological properties (vascular occlusion and bilateral involvement), and the most important aetiology (idiopathic) [4)]. The incidence rate of moyamoya disease in Northeast Asia is higher than that in other regions, especially in Japan, Korea, and China [5)]. The incidence and prevalence of MMD in mainland China as 0.59 and 1.01 per 100 000 person-years[6)], respectively. MMD maintains a classical pattern of bimodal

age distribution. The first peak occurs around the age of five and the second one around the age of 40. The incidence rate of women is higher than that of men (female-to-male ratios is 1.12)[6].

The pathogenesis of moyamoya disease is not clear and may be related to genetics, immunity, inflammation and other factors. Ring finger protein 213 (RNF213) has recently been identified as a susceptibility gene for moyamoya disease [7,8]. Studies have confirmed that the apoptosis-inducing function of the RNF213 gene may be negatively regulated by its ubiquitin ligase, which is highly related to the occurrence of moyamoya disease [9]. However, Sonobe et al. found that mice lacking the RNF213 gene did not spontaneously produce moyamoya disease, which indicated that the loss of function of RNF213 could not fully induce moyamoya disease [10]. Therefore, although RNF213 may be a pathogenic factor of moyamoya disease, its specific mechanism in the pathogenesis of moyamoya disease is still unclear. Moyamoya disease is associated with the class I and class II genes of human leukocyte antigen (HLA), although the related genetic genes differ significantly among different races [11]. In moyamoya disease, when smooth muscle proliferates, macrophages and T lymphocytes infiltrate the intimal surface, resulting in intimal hyperplasia and lumen stenosis, which may be the main inflammatory mechanism of the disease [12]. As multimodal three-dimensional angiography technology matures, our understanding of moyamoya disease and the standardization of diagnostic standards have improved, which has increased the worldwide detection rate of moyamoya disease year by year. The treatment of moyamoya disease mainly revolves around surgical intervention. Direct and indirect revascularization surgeries are performed to improve blood circulation in the affected region[13]. However, a clear conclusion has not been reached on the pathogenesis and evolution of moyamoya disease, and there is still a lack of effective biomarkers and molecular targeted therapies.

MicroRNAs (miRNAs) are single-stranded RNA molecules that measure approximately 21–23 nucleotides in length and participate in a lot of biological processes. Exosomes play an important role in many physiological and pathological processes, such as antigen presentation in immunity, tumour growth and migration, and tissue damage repair. Exosomes secreted by different cells have different components and functions and can be used as biomarkers for disease diagnosis. Exosomes have a lipid bilayer membrane structure, which can protect their coated substances and target specific cells or tissues; therefore, they can act as a targeted drug delivery system [14]. Studies have found that exosomal miRNAs derived from cerebrospinal fluid of moyamoya disease patients may serve as a novel diagnostic biomarker for diagnosis [15]. Therefore, this study analysed the miRNAs expressed in the exosomes from plasma samples from moyamoya disease patients and healthy individuals via next-generation sequencing (NGS). This analysis quantified the expression profile of exosomal miRNAs and identified statistically correlated miRNAs to determine pathways that potentially mediate the pathogenesis and biomarkers of moyamoya disease.

2 Methods

2.1 Patients

Nine patients diagnosed with moyamoya disease by digital subtraction angiography were enrolled at Peking University Shenzhen Hospital from December 2020 to March 2021. The diagnostic criteria of moyamoya disease were on the basis of the guidelines published in 2012 by the Research Committee on the Spontaneous Occlusion of the Circle of Willis of the Ministry of Health and Welfare, Japan. These patients were between 20 and 65 years old and definitely moyamoya disease, accompanied by bleeding or ischemic comorbidities based on clinical symptoms and imaging diagnosis (4 males and 5 females). Ten healthy individuals were recruited from the physical examination centre as the control group with the criteria that no obvious intracranial disease diagnosed by CT and no central nervous system disease related history. All patients signed an informed agreement. For peripheral blood collection, 3 mL of peripheral blood from enrolled participants was collected into 5-mL K2EDTA Vacutainer tubes (Junnuo, Chengwu, China). The study was approved by the medical ethics committee of Peking University Shenzhen Hospital.

2.2 Isolation and identification of exosomes

The plasma supernatant was collected and centrifuged at 3500 g at 4°C for 10 min, and then the supernatant was centrifuged at 12000 g at 4°C for 10 min. The precipitate was discarded, and the supernatant was collected for exosome extraction. Exosomes were extracted based on exoQuick precipitation using an ExoQuick precipitation system (System Biosciences Inc., CA, United States). Briefly, the plasma supernatant was added to the exosome extraction reagent and centrifuged at 1500 × g for 10 min at 4°C to pellet the exosomes. The exosomes were resuspended in 10 mM PBS at four times the volume of supernatant. A nanoparticle tracking analysis (NTA) and transmission electron microscopy (TEM) were used to identify the exosome features.

2.3 Western Blot Analysis

Exosomes were dissolved in RIPA buffer (ASPEN, Wuhan, China), and the protein concentrations were determined using a BCA Protein Assay Kit (ASPEN, Wuhan, China). Protein extracts were separated by 10% sodium dodecyl sulfate polyacrylamide gel electrophoresis (SDS–PAGE) and blotted onto a polyvinylidene difluoride (PVDF) membrane (Millipore, MA, United States). The membranes were incubated with CD63 (Abcam, ab217345) and CD81 (Abcam, ab109201) primary antibodies at 4°C overnight after blocking with 5% BSA. Next, the corresponding secondary antibodies were incubated at room temperature for 1 h. The protein bands were visualized using Immobilon ECL Ultra Western HRP Substrate (ASPEN, Wuhan, China). A Tanon-5500 Chemiluminescent Imaging System (Tanon Science & Technology, Shanghai, China) was used for visualized imaging.

2.3.1 RNA library construction and sequencing

First, TRIzol reagent (Invitrogen Life Technologies, Carlsbad, CA) was used to extract total RNA from the exosome pellets following the manufacturer’s instructions. The total RNA concentration and quality were

quantified using a Qubit3 Fluorometer (Thermo Fisher Scientific, MA, United States) and an Agilent Bioanalyser 2100 (Agilent Technologies, CA, United States).

The small RNA library was constructed according to the QIAseq miRNA Library kit (QIAGEN, Germany). Approximately 100 ng of total RNA was used to prepare the miRNA library, and it was supplemented with water to 20 μL. The library was constructed to ligate at the 3' and 5' ends of small RNA. Then, reverse transcription of the sample was started to obtain cDNA. QIAseq miRNA NGS beads were used to wash cDNA several times according to the manufacturer's instructions. The concentration and quality of the small RNA library were analysed using an Agilent Bioanalyser 2100 (Agilent Technologies, CA, United States). The qualifying small RNA libraries were sequenced on a HiSeq 2500 (Illumina, San Diego, USA).

2.4 Data Processing and Bioinformatics Analysis

The small RNA sequencing raw data were processed to estimate microRNA expression. In brief, the adapter sequences were trimmed using cut adapt software, and then the Q20, Q30, and GC content of the clean data were calculated. Reads longer than 17 nt and smaller than 35 nt were aligned to human mature microRNA (miRBase release 22.1) using FANSe [16)]. The expression of microRNAs (miRNAs) was represented by the RPM value (RPM = read Count*1,000,000/sum of mapped read Count). Differential expression analyses of two groups were performed using the edgeR package. The P values were adjusted using Benjamini and Hochberg's approach for controlling the false discovery rate. MiRNAs with an adjusted P value < 0.01 and fold change > 2 found by edgeR were considered differentially expressed. The miRNA targets were predicted using the prediction website TargetScan (http://www.targetscan.org/vert_71/). A Gene ontology (GO) enrichment analysis was performed via topGO, and a Kyoto Encyclopaedia of Genes and Genomes (KEGG) pathway analysis was performed using clusterProfiler (kobas2.0-20150126).

2.5 Real-time quantitative PCR (RT-QPCR)

The miRNA expression levels were assessed by qRT–PCR. Total RNA and total RNA were reverse transcribed to cDNA using the PrimeScript First Strand cDNA Synthesis Kit (Takara, Beijing, China). RT-QPCR was carried out using 2X SYBR green qPCR mix (Takara, Beijing, China) and an ABI 7900HT sequence system (Thermo Fisher Scientific, Inc.). The reactions were incubated at 94°C for 3 min, followed by 40 cycles at 95°C for 15 s and 62°C for 40 s. The primer sequences for the four miRNAs are shown in Table 1. U6 was used as an internal control of miRNAs. Statistical analyses of the results were performed using the $2-\Delta\Delta CT$ relative quantification method.

Table 1
Information of validated miRNAs.

miRNA	Primers (5′— 3′)
hsa-miR-1306-5p	CCACCTCCCCTGCAAACGTCCA
hsa-miR-22-3p	AAGCTGCCAGTTGAAGAACTGT
hsa-miR-34a-5p	TGGCAGTGTCTTAGCTGGTTGT
hsa-miR-489-3p	GTGACATCACATATACGGCAGC
hsa-miR-501-3p	AATGCACCCGGGCAAGGATTCT
has-miR-196b-5p	TAGGTAGTTTCCTGTTGTTGGG
has-miR-19a-3p	TGTGCAAATCTATGCAAAACTGA
has-miR-320b	AAAAGCTGGGTTGAGAGGGCAA
has-miR-485-3p	GTCATACACGGCTCTCCTCTCT
has-miR-487b-3p	AATCGTACAGGGTCATCCACTT

2.6 Statistical analysis

Student's t test was applied to the RT-QPCR analysis results to compare the different groups using GraphPad Prism 5.0. ROC curves and AUC values were determined using edgeR package. GO and KEGG pathway analyses were assessed by Fisher's exact test to identify significant results using the edgeR package. P values < 0.05 were significant.

3 Results

3.1 Characterization of exosomes obtained from moyamoya disease patient plasma

The clinical information of the sample is shown in Table 2. There is no significant difference between the age and gender of the patient. According to whether the patient will see smoke-like changes in the brain during the digital subtraction cerebrovascular angiography examination, we can distinguish patients with moyamoya disease from patients with non-moyamoya disease. For example, Figs. 1A and B show a patient with the same hemorrhagic moyamoya disease (bilateral), characterized by cerebral hemorrhage, occlusion of the end of the internal carotid artery on the right side, and smoke vessel formation). Figures 1C and D are the same healthy person, showing normal cerebral blood vessels. To characterize exosomes derived from moyamoya disease patient plasma, transmission electron microscopy, nanoparticle tracking analysis and western blotting were used to characterize exosome diameters and protein markers. CD63 and CD81 are protein markers of exosomes, and CD63 and CD81 are protein markers of exosomes, and

were detected in NC exosomes, MMD exosomes and plasma by Western blotting analysis, it confirmed that we isolated exosomes (Fig. 1E). Transmission electron microscopy showed a typical rounded morphology with a sagged double membrane (Fig. 1F). The nanoparticle tracking analysis further confirmed that the exosome isolated from moyamoya disease patients and health people were 30–150 nm in diameter (Fig. 1G). These results indicated that exosomes were successfully purified from all plasma samples.

Table 2
Clinical information of the samples

	NC	MMD	*P*-value
Male sex	5(50)	5(56%)	0.967
Age	46.1 ± 6.4	48.9 ± 12.1	0.603
WBC($\times 10^9$)	6.08 ± 1.24	7.23 ± 1.37	0.169
RBC($\times 10^9$)	4.45 ± 0.32	4.45 ± 0.41	0.967
Hb(mmol/L)	133 ± 7.1	132 ± 13	0.791
Glu(mmol/L)	5.31 ± 0.62	5.21 ± 0.65	0.729
K^+(mmol/L)	4.02 ± 0.21	3.95 ± 0.21	0.456
Na^+(mmol/L)	139.7 ± 3.4	141.1 ± 2.5	0.306
ALT(U/L)	19.5 ± 6.6	24.45 ± 15.18	0.364
TB(umol/L)	9.38 ± 3.03	8.58 ± 3.01	0.561
DB(umol/L)	1.92 ± 0.19	1.75 ± 0.39	0.232
TC(mg/DL)	3.63 ± 1.03	3.88 ± 1.57	0.678
TG(mg/DL)	1.41 ± 0.69	1.54 ± 0.87	0.737
HDL(mg/DL)	0.99 ± 0.07	0.97 ± 0.27	0.85
LDL(mg/DL)	2.88 ± 0.63	3.02 ± 0.77	0.662

Table 3
Sequencing data output statistics and quality control

Sample Name	Raw Reads	Clean Reads	Q20	Q30	GC%
MMD1	13394601	11470036	0.994038	0.979452	0.541002
MMD2	16789838	15597279	0.993253	0.977721	0.543984
MMD3	19767133	14471822	0.993802	0.979251	0.541744
MMD4	10192610	8096998	0.994197	0.979526	0.552548
MMD5	13430381	11318666	0.993618	0.978735	0.542509
MMD6	19573465	17755102	0.994607	0.98019	0.538964
MMD7	20702651	17529882	0.99429	0.980239	0.527753
MMD8	18527733	17109638	0.99283	0.977045	0.502724
MMD9	21319758	20473411	0.993715	0.978213	0.487527
NC1	12058148	11396788	0.984477	0.949508	0.552691
NC2	37649858	36311886	0.990424	0.966974	0.548631
NC3	21111513	18796751	0.989343	0.965364	0.566005
NC4	35556828	29895610	0.986185	0.954861	0.548253
NC5	11792452	11097666	0.985199	0.951597	0.559581
NC6	15052720	4073973	0.992414	0.974378	0.585476
NC7	11093372	5542318	0.992088	0.973208	0.580912
NC8	10618213	7722455	0.991523	0.972106	0.588273
NC9	11282238	7778548	0.992302	0.974028	0.582235
NC10	30780243	20582756	0.992305	0.974105	0.583265

3.2 GO and KEGG analyses of the target genes of differentially expressed miRNAs

Next, the raw data were obtained by high-throughput sequencing. The connectors at both ends of the reads were cut off by cutadapt software, and the reads with lengths greater than 17 nt were retained. The basic quality information on the reads showed that they can be used for subsequent data analyses (Table 3). A total of 1002 differentially expressed miRNAs were identified based on an false discovery rate < 0.01 and fold change > 2, and they included 585 upregulated and 417 downregulated miRNAs (Fig.

2A). Target genes of differential miRNAs were predicted via the TargetScan database. A gene ontology (GO) analysis and Kyoto Encyclopaedia of Genes and Genomes (KEGG) pathway analysis were conducted to explore the function of the target genes of differentially expressed miRNAs. According to the GO analysis, the results indicated that these decreased expressed miRNAs were primarily associated with biological process terms, including regulation of cellular metabolic process, regulation of cellular process, cellular macromolecule metabolic process(Fig. 2B). They were also were enriched in cellular component terms, including nucleoplasm, intracellular part, intracellular(Fig. 2C), and molecular function terms, including transcription regulatory region sequence-specific DNA binding and regulatory region nucleic acid binding(Fig. 2D). These increased expressed miRNAs were primarily associated with biological process terms, including nervous system development, positive regulation of cellular process, positive regulation of biological process(Fig. 3A); cellular component terms, including cytoplasm, intracellular, and intracellular part(Fig. 3B), and molecular function terms, including protein binding and regulatory region nucleic acid binding (Fig. 3C).The KEGG pathway analysis for these target genes showed that they were mainly enriched in axon guidance, regulation of the actin cytoskeleton and the MAPK signalling pathway (Fig. 3D). There were 63 exosomal miRNAs involved in the axon guidance, regulation of actin cytoskeleton and MAPK signaling pathway (Fig. 4A). Among them, the different target genes of 59 exosomal miRNAs were associated with the three pathways at the same time, especially with regulation of actin cytoskeleton (Fig. 4B). Function predictions and pathway analyses of target genes of differentially expressed miRNAs could provide insights to help regulate the actin cytoskeleton in the pathogenesis of moyamoya disease.

3.3 Prognosis of potential biomarkers by the receiver operating characteristic curve and area under curve

To further screen potential biomarkers of moyamoya disease, the area under the curve of the receiver operating characteristic (ROC) curve was used to evaluate the sensitivity and specificity of biomarkers for predicting events. The sensitivity and specificity of each miRNA were determined by the optimal threshold of the area under the curve (AUC). AUC of ROC were carried out determining the diagnostic values of these 63 miRNAs involved in the axon guidance, regulation of actin cytoskeleton and MAPK signaling pathway. Ten miRNAs (miR-1306-5p, miR-196b-5p, miR-19a-3p, miR-22-3p, miR-320b, miR-34a-5p, miR-485-3p, miR-489-3p, miR-501-3p, and miR-487b-3p) had significantly differentiated moyamoya disease patients from healthy controls based on an AUC value above 0.9 and sensitivity and specificity above 0.8 (Fig. 5). To further explore the expression of these exosomal miRNAs as potential biomarkers of moyamoya disease, RT-QPCR was performed to detect randomly the levels of these exosomal miRNAs extracted from the plasma samples of 9 moyamoya disease patients and 10 healthy individuals. These ten microRNAs showed the same expression patterns obtained from the high-throughput sequencing analysis. Hsa-miR-34a-5p, Hsa-miR-19a-3p, miR-22-3p, miR-196a-5p, miR-320b, miR-485-3p, miR-487b-3p, and miR-501-3p were up-regulated, and miR-489-3p and hsa-miR-1306-5p were downregulated (Fig. 6). These results indicated that these exosomal miRNAs are potential biomarkers that may participate in the

regulation of the actin cytoskeleton in moyamoya disease. In summary, the analysis of the differentially expressed exosomal miRNAs in plasma revealed that they may have a functional role in the pathogenesis of moyamoya disease.

4 Discussion

In this study, we established a method for screening moyamoya disease-specific miRNAs from plasma exosomes. Although many studies have shown that secreted miRNA may represent potential biomarkers for many diseases, few studies have analysed the role of plasma-secreted miRNA in moyamoya disease [15)]. To the best of our knowledge, this is the first study which successfully obtain exosomal miRNAs from a large number of plasma miRNAs and conduct a high-throughput sequencing analysis of the miRNAs, which can be used as biomarkers of clinical moyamoya disease and may be involved in the pathogenesis of moyamoya disease. Moyamoya disease is a disease of the central nervous system, and the molecular changes in cerebrospinal fluid may reflect the molecular conditions of the central nervous system[17)]. But extracting cerebrospinal fluid from peripheral blood is not convenient [18)]. Moreover, cerebrospinal fluid cannot be extracted for patients in certain age groups, and certain restrictions may also apply [19,20)]. Therefore, biomarkers in peripheral blood represent a valuable method of performing humoral diagnoses. Through the miRNA analysis of peripheral blood exosomes, we can develop a noninvasive rapid detection kit for the early diagnosis of moyamoya disease.

In this study, the top three signalling pathways enriched by the target genes of the differentially expressed exosomal miRNAs were axon guidance, regulation of the actin cytoskeleton and the MAPK signalling pathway. Exosome studies have the potential to determine intercellular communication and organ homeostasis as well as unknown cellular and molecular mechanisms in diseases. The biogenesis of exosomes involves their origin in cells and their interactions with other cells and organelles. The contents of exosomes can reflect disease conditions to a certain extent [21)]. A proteomic analysis of the serum exosomes from patients with moyamoya disease showed that 859 shared proteins were detected in the serum exosomes from patients with ischaemic and haemorrhagic moyamoya disease, and 231 of which were different from those in the healthy controls. A bioinformatics analysis of these proteins revealed a protein imbalance and actin dynamics disorder related to cell growth and maintenance in moyamoya disease [22)]. Ren et al.[23)] found both MMD patient and Neo1 (neogenin) mutant mice exhibited altered gene expression in their cortex in proteins critical for axon guidance ,suggesting that Neo1 relevant axon guidance pathway may play important roles in regulating MMD-like vasculopathy. Previous studies have shown that the MAPK signaling pathway plays an important role in the pathogenesis of moyamoya disease[24)]. These finding further supported our results that plasma exosomal miRNAs, as potential biomarkers, which contributes to the pathogenesis of moyamoya disease.

Moreover, we found miR-1306-5p, miR-196b-5p, miR-19a-3p, miR-22-3p, miR-320b, miR-34a-5p, miR-485-3p, miR-489-3p, miR-487b-3p, and miR-501-3p had high sensitivity and specificity for predicting moyamoya disease, and may serve as biomarkers of moyamoya disease. Transfection of miR-1306-5p

mimics eliminated the inhibitory effect of SNHG7-003 overexpression on the proliferation and migration of vascular smooth muscle cells [25]. MiR-34a directly regulates the expression of the target gene sirtuin 1 (SIRT1), which interacts with C2DAT1 to affect the proliferation and migration of vascular smooth muscle cells [26]. MiR-34a-5p participates in autophagy of human coronary artery endothelial cells induced by chronic intermittent hypoxia through the Bcl-2/Beclin1 signalling transduction pathway [27]. MiRNA-34a-5p reduces the expression of VEGFA in endometrial stem cells involved in the pathogenesis of endometriosis [28]. In addition, microRNA-34a promotes endothelial dysfunction and mitochondrial-mediated apoptosis in a mouse model of acute lung injury [29]. Under hypoxia, an inhibitor of miR-485-3p can promote the proliferation of human microvascular endothelial cells [30]. High expression of exosomal miR-501–3p promotes vascular sclerosis [31]. miR-22-3p can regulate human artery vascular smooth muscle cell proliferation and migration by targeting HMGB1, and may be therapeutic targets in the treatment of human arteriosclerosis obliterans[32]. Dysregulation Serum miR-19a-3p is a Diagnostic Biomarker for Asymptomatic Carotid Artery Stenosis and a Promising Predictor of Cerebral Ischemia Events[33]. miR-320b is a specific serum marker for carotid atherosclerosis and vulnerable plaque, which can be used to assist in the diagnosis of cerebrovascular diseases[34]. These previous results support the findings of our study, in which the imbalance of miRNA expression has an impact on moyamoya disease, but it still needs to be confirmed by protein level and mechanism-based analysis. miR-196b-5p, miR-489-3p, miR-489-3p are first reported to be related to moyamoya disease, and more studies are needed to explore the mechanism of action of these miRNAs on moyamoya diseas.

5 Limitations And Future Directions

Although much of the data revealed by this work is promising, there are clearly a number of limitations inherent to this study. First, a challenge is the rarity of this disease, and it takes enough time to collect large amounts of samples. If the data is to be more reliable, it is ideal to explore the relationship between these miRNAs and moyamoya disease in more clinical samples. Secondly, there is a lack of further verification of the influence of miRNA on the pathogenesis of moyamoya disease. Next, cell or animal experiments should be carried out to study the mechanism of miRNA on moyamoya disease, so as to provide more basic evidence for the clinical application of miRNA in the diagnosis and treatment of moyamoya disease.

6 Conclusions

In this study, we identified for the first time the miRNA expression profile of plasma exosomes in patients with moyamoya disease by high-throughput sequencing and found that the regulation of the actin cytoskeleton pathway may be involved in the pathogenesis of moyamoya disease. Moreover, this study found that some exosomal miRNAs, such as miR-1306-5p, miR-196b-5p, miR-19a-3p, miR-22-3p, miR-320b, miR-34a-5p, miR-485-3p, miR-489-3p, miR-487b-3p, and miR-501-3p might serve as are potential biomarkers for the diagnosis of moyamoya disease in future studies and mediate the pathogenesis.

Declarations

7. Conflict of Interest

The author declares that there is no conflict of interest.

8. Author Contributions

Da Huang: Conceptualization, Methodology, Writing - Original Draft. Hui Qi: Methodology, Formal analysis, Writing - Original Draft. Hongchun Yang Investigation, Visualization. Meng chen: Software, Formal analysis.

9. Funding

This work was supported by Shenzhen Municipal Health and Family Planning System Scientific Research Project No. SZXJ2017052.

10. Acknowledgments

Thanks for every patient participated in this study. It is their disease data that lays the foundation for the subsequent treatment of patients.

11. Data availability statements

The data that support the findings of this study are available from the corresponding author upon reasonable request. The raw data files of high-throughput sequencing were uploaded to https://zenodo.org/.DOI10.5281/zenodo.5800422.

12. Ethics approval and consent to participate

The study was approved by the medical ethics committee of Peking University Shenzhen Hospital. All ethics procedures conformed with the principles of the 1964 Declaration of Helsinki and its latest 2008 amendments. Informed consent has been obtained from all subjects and/or their legal guardians.

13. Consent for publication

All participants in the study agreed to be published.

References

1. Scott RM, Smith ER. Moyamoya disease and moyamoya syndrome. The New England journal of medicine. Mar 19 2009;360(12):1226–1237.
2. Suzuki J, Takaku A. Cerebrovascular "moyamoya" disease. Disease showing abnormal net-like vessels in base of brain. Archives of neurology. Mar 1969;20(3):288–299.
3. Fujimura M, Bang OY, Kim JS. Moyamoya Disease. Frontiers of neurology and neuroscience. 2016;40:204–220.
4. Rupareliya C, Lui F. Moyamoya Disease. *StatPearls*. Treasure Island (FL)2021.
5. Hu J, Luo J, Chen Q. The Susceptibility Pathogenesis of Moyamoya Disease. World neurosurgery. May 2017;101:731–741.
6. Sun Y, Zhou G, Feng J, et al. Incidence and prevalence of moyamoya disease in urban China: a nationwide retrospective cohort study. Stroke and Vascular Neurology. 2021:svn-2021-000909.
7. Liu W, Morito D, Takashima S, et al. Identification of RNF213 as a susceptibility gene for moyamoya disease and its possible role in vascular development. PloS one. 2011;6(7):e22542.
8. Sato-Maeda M, Fujimura M, Rashad S, et al. Transient Global Cerebral Ischemia Induces RNF213, a Moyamoya Disease Susceptibility Gene, in Vulnerable Neurons of the Rat Hippocampus CA1 Subregion and Ischemic Cortex. Journal of stroke and cerebrovascular diseases: the official journal of National Stroke Association. Sep 2017;26(9):1904–1911.
9. Takeda M, Tezuka T, Kim M, et al. Moyamoya disease patient mutations in the RING domain of RNF213 reduce its ubiquitin ligase activity and enhance NFkappaB activation and apoptosis in an AAA + domain-dependent manner. Biochemical and biophysical research communications. May 7 2020;525(3):668–674.
10. Sonobe S, Fujimura M, Niizuma K, et al. Temporal profile of the vascular anatomy evaluated by 9.4-T magnetic resonance angiography and histopathological analysis in mice lacking RNF213: a susceptibility gene for moyamoya disease. Brain research. Mar 13 2014;1552:64–71.
11. Inoue TK, Ikezaki K, Sasazuki T, Matsushima T, Fukui M. Analysis of class II genes of human leukocyte antigen in patients with moyamoya disease. Clinical neurology and neurosurgery. Oct 1997;99 Suppl 2:S234-237.
12. Mikami T, Suzuki H, Komatsu K, Mikuni N. Influence of Inflammatory Disease on the Pathophysiology of Moyamoya Disease and Quasi-moyamoya Disease. Neurologia medico-chirurgica. Oct 15 2019;59(10):361–370.
13. Starke RM, Komotar RJ, Connolly ES. Optimal surgical treatment for moyamoya disease in adults: direct versus indirect bypass. Neurosurgical focus. Apr 2009;26(4):E8.
14. Farooqi AA, Desai NN, Qureshi MZ, et al. Exosome biogenesis, bioactivities and functions as new delivery systems of natural compounds. Biotechnology advances. Jan - Feb 2018;36(1):328–334.
15. Wang G, Wen Y, Faleti OD, et al. A Panel of Exosome-Derived miRNAs of Cerebrospinal Fluid for the Diagnosis of Moyamoya Disease. Frontiers in neuroscience. 2020;14:548278.

16. Zhang G, Fedyunin I, Kirchner S, Xiao C, Valleriani A, Ignatova Z. FANSe: an accurate algorithm for quantitative mapping of large scale sequencing reads. Nucleic acids research. Jun 2012;40(11):e83.
17. Farooq S, Testai FD. Neurologic Complications of Sickle Cell Disease. Current neurology and neuroscience reports. Feb 28 2019;19(4):17.
18. Gaetani L, Paolini Paoletti F, Bellomo G, et al. CSF and Blood Biomarkers in Neuroinflammatory and Neurodegenerative Diseases: Implications for Treatment. Trends in pharmacological sciences. Dec 2020;41(12):1023–1037.
19. Matzneller P, Burian A, Zeitlinger M, Sauermann R. Understanding the Activity of Antibiotics in Cerebrospinal Fluid in vitro. Pharmacology. 2016;97(5–6):233–244.
20. Rahimi J, Woehrer A. Overview of cerebrospinal fluid cytology. Handbook of clinical neurology. 2017;145:563–571.
21. Kalluri R, LeBleu VS. The biology, function, and biomedical applications of exosomes. Science. Feb 7 2020;367(6478).
22. Wang X, Han C, Jia Y, Wang J, Ge W, Duan L. Proteomic Profiling of Exosomes From Hemorrhagic Moyamoya Disease and Dysfunction of Mitochondria in Endothelial Cells. Stroke. Aug 2 2021:STROKEAHA120032297.
23. Ren X, Yao L-L, Pan J-X, et al. Linking cortical astrocytic neogenin deficiency to the development of Moyamoya disease–like vasculopathy. *Neurobiology of Disease.* 2021/07/01/ 2021;154:105339.
24. Sudhir BJ, Keelara AG, Venkat EH, Kazumata K, Sundararaman A. The mechanobiological theory: a unifying hypothesis on the pathogenesis of moyamoya disease based on a systematic review. Neurosurgical focus. 2021;51(3):E6.
25. Zheng J, Tan Q, Chen H, et al. lncRNASNHG7003 inhibits the proliferation, migration and invasion of vascular smooth muscle cells by targeting the miR13065p/SIRT7 signaling pathway. International journal of molecular medicine. Feb 2021;47(2):741–750.
26. Wang H, Jin Z, Pei T, et al. Long noncoding RNAs C2dat1 enhances vascular smooth muscle cell proliferation and migration by targeting MiR-34a-5p. Journal of cellular biochemistry. Mar 2019;120(3):3001–3008.
27. Lv X, Wang K, Tang W, et al. miR-34a-5p was involved in chronic intermittent hypoxia-induced autophagy of human coronary artery endothelial cells via Bcl-2/beclin 1 signal transduction pathway. Journal of cellular biochemistry. Nov 2019;120(11):18871–18882.
28. Ma Y, Huang YX, Chen YY. miRNA34a5p downregulation of VEGFA in endometrial stem cells contributes to the pathogenesis of endometriosis. Molecular medicine reports. Dec 2017;16(6):8259–8264.
29. Shah D, Das P, Alam MA, et al. MicroRNA-34a Promotes Endothelial Dysfunction and Mitochondrial-mediated Apoptosis in Murine Models of Acute Lung Injury. American journal of respiratory cell and molecular biology. Apr 2019;60(4):465–477.
30. Hu C, Bai X, Liu C, Hu Z. Long noncoding RNA XIST participates hypoxia-induced angiogenesis in human brain microvascular endothelial cells through regulating miR-485/SOX7 axis. American

journal of translational research. 2019;11(10):6487–6497.

31. Toyama K, Igase M, Spin JM, et al. Exosome miR-501-3p Elevation Contributes to Progression of Vascular Stiffness. Circulation reports. Feb 17 2021;3(3):170–177.
32. Huang S, Wang M, Wu W, et al. Mir-22-3p Inhibits Arterial Smooth Muscle Cell Proliferation and Migration and Neointimal Hyperplasia by Targeting HMGB1 in Arteriosclerosis Obliterans. Cellular Physiology and Biochemistry. 2017;42(6):2492–2506.
33. Liu X, Zheng X, Wang Y, Liu J. Dysregulation Serum miR-19a-3p is a Diagnostic Biomarker for Asymptomatic Carotid Artery Stenosis and a Promising Predictor of Cerebral Ischemia Events. Clinical and Applied Thrombosis/Hemostasis. 2021;27:10760296211039287.
34. Zhang R, Qin Y, Zhu G, Li Y, Xue J. Low serum miR-320b expression as a novel indicator of carotid atherosclerosis. *Journal of Clinical Neuroscience.* 2016/11/01/ 2016;33:252–258.

Figures

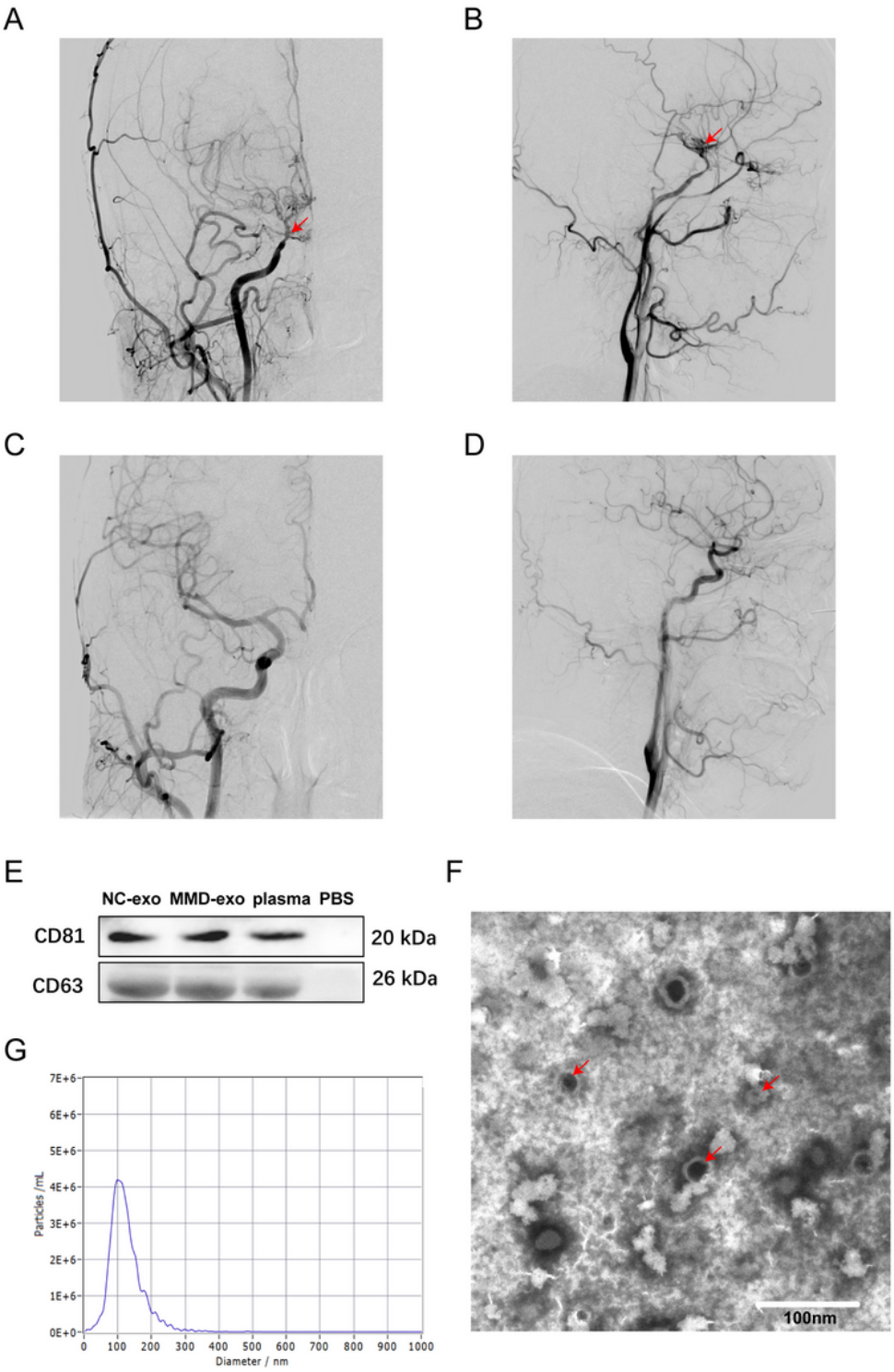

Figure 1

Digital subtraction angiography (DSA) images and characterization of exosomes in plasma of moyamoya disease patients. (A-B) Digital subtraction angiography (DSA) images of moyamoya disease patients. The arrows on the pictures showed the narrowing/stenosis of the carotid artery that causes the moyamoya disease. (C-D) Digital subtraction angiography (DSA) images of non-moyamoya disease patients. A, C are standard anterior positions, B, D are standard lateral positions. (E) The protein levels of

CD81 and CD63 in exosomes were analyzed by western blotting. (F) Transmission electron microscopy image of a mixture of NC and MMD exosomes. The arrows on the pictures showed exosomes. Scale bar, 100 nm. (G) Size distribution of exosomes determined by nanoparticle tracking analysis. NC-exo, exosomes from normal control. MMD-exo, exosomes from moyamoya disease.

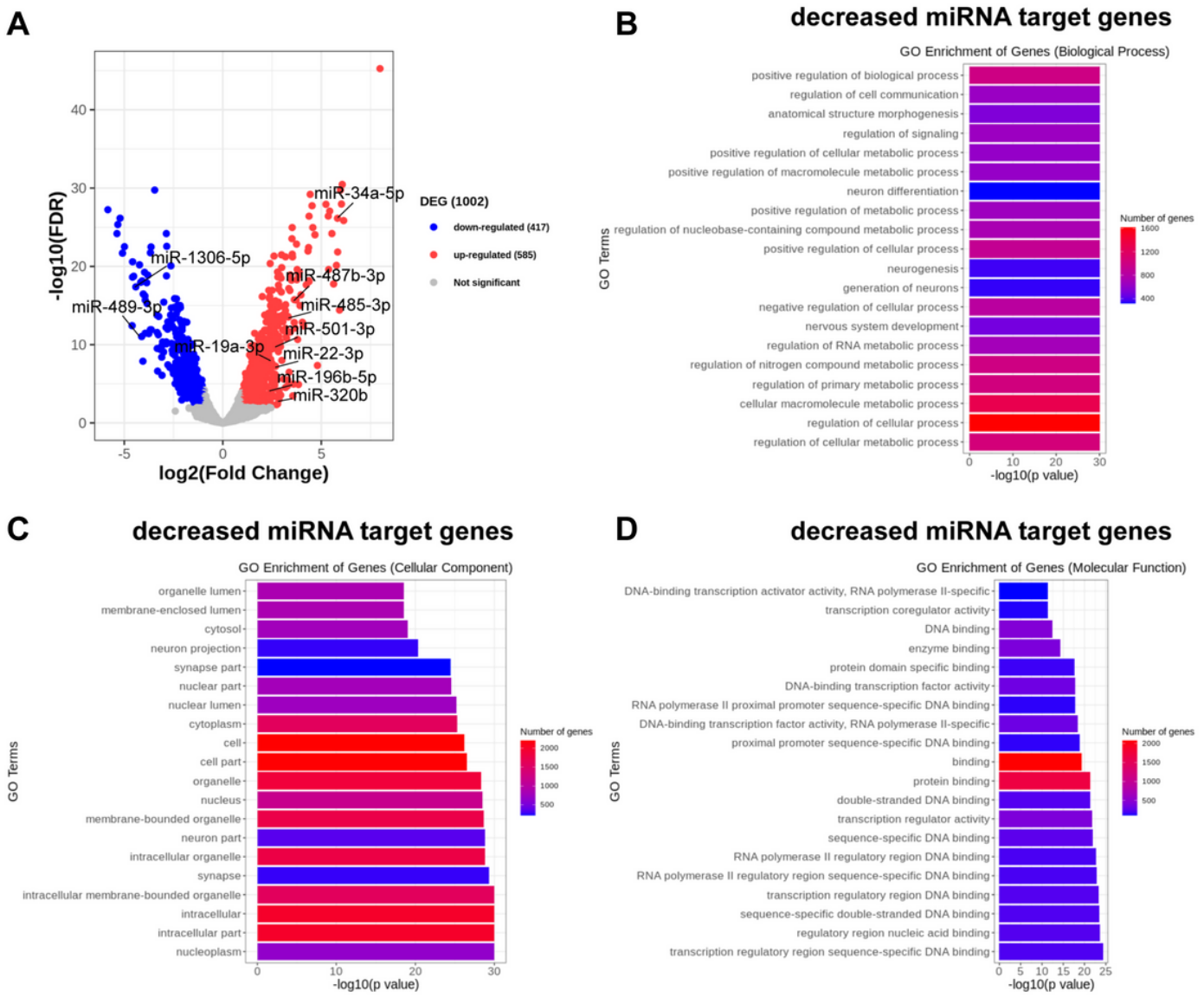

Figure 2

The expression of miRNAs analysis and Enrichment analysis of target genes of significantly differ-expressed miRNAs. (A) Volcano plot of significantly differ-expressed miRNAs between moyamoya disease patients and healthy control group. (B-D) GO enrichment analysis of target genes of decreased expressed miRNAs in biological process (B), cellular components (C), and molecular function (D). NC, normal control. MMD, moyamoya disease.

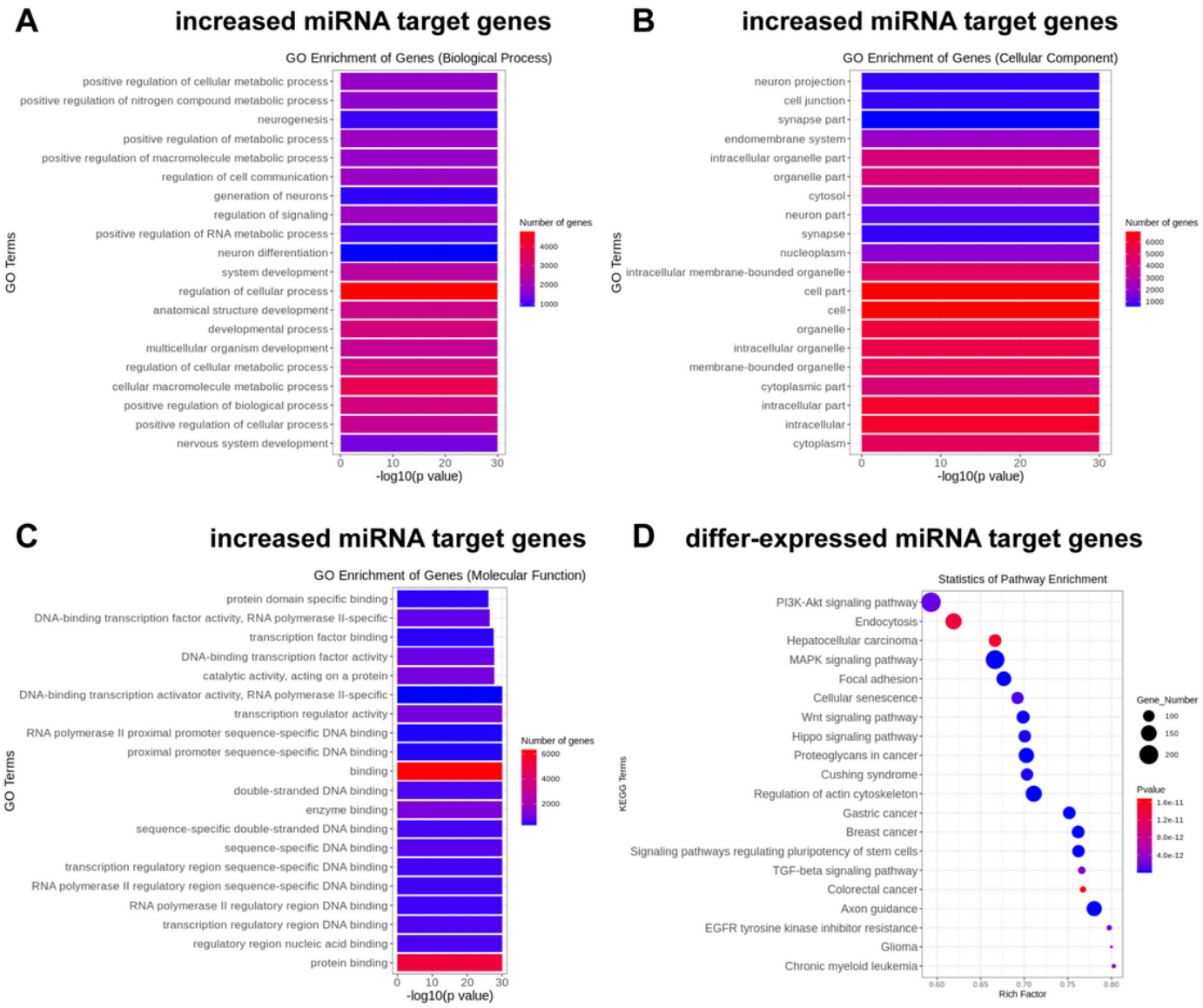

Figure 3

Enrichment analysis of target genes of significantly differ-expressed miRNAs. (A-C) GO enrichment analysis of target genes of increased expressed miRNAs in biological process (A), cellular components (B), and molecular function (C). (D) KEGG enrichment analysis of target genes of differentially expressed miRNAs. NC, normal control. MMD, moyamoya disease.

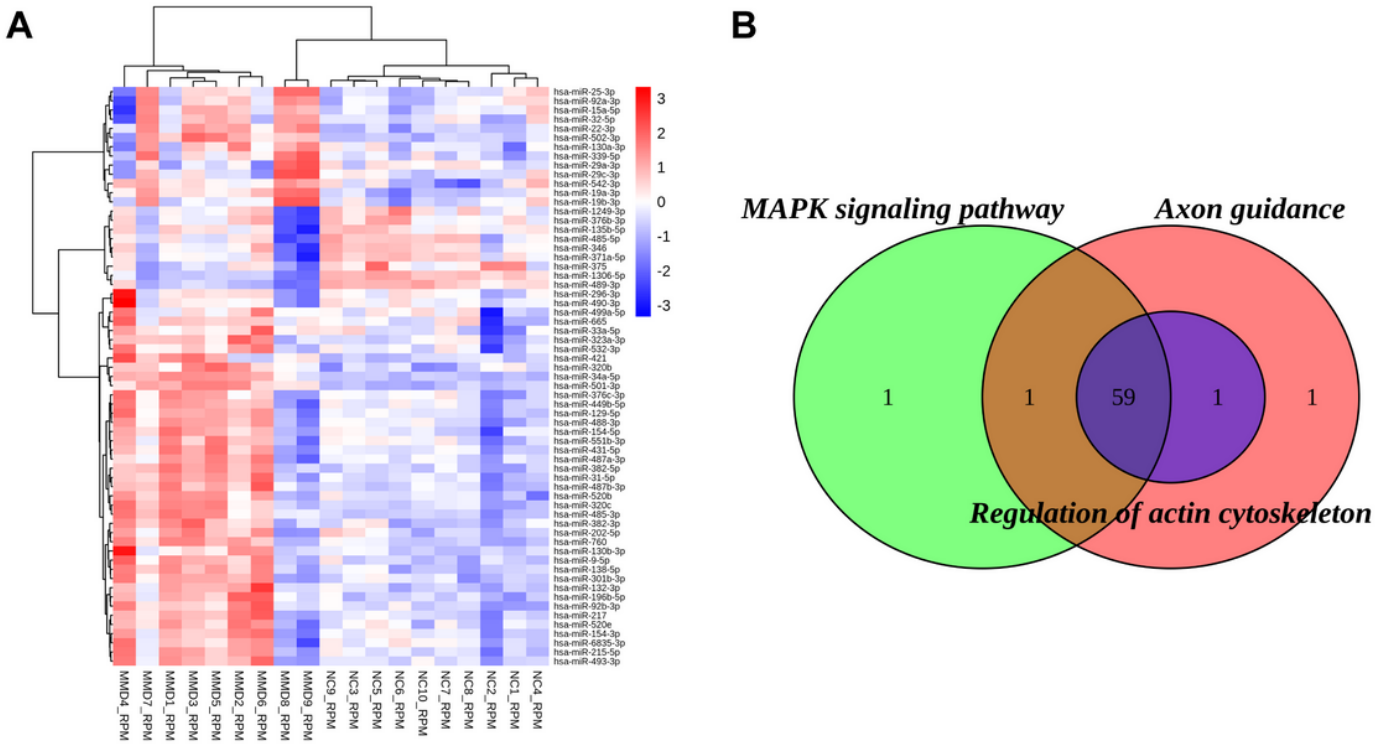

Figure 4

significantly differ-expressed miRNAs analysis. (A) Heatmap of differentially expressed miRNAs involved in in the axon guidance, regulation of actin cytoskeleton and MAPK signaling pathway. (B) Venn of differentially expressed miRNAs involved in in the axon guidance, regulation of actin cytoskeleton and MAPK signaling pathway.

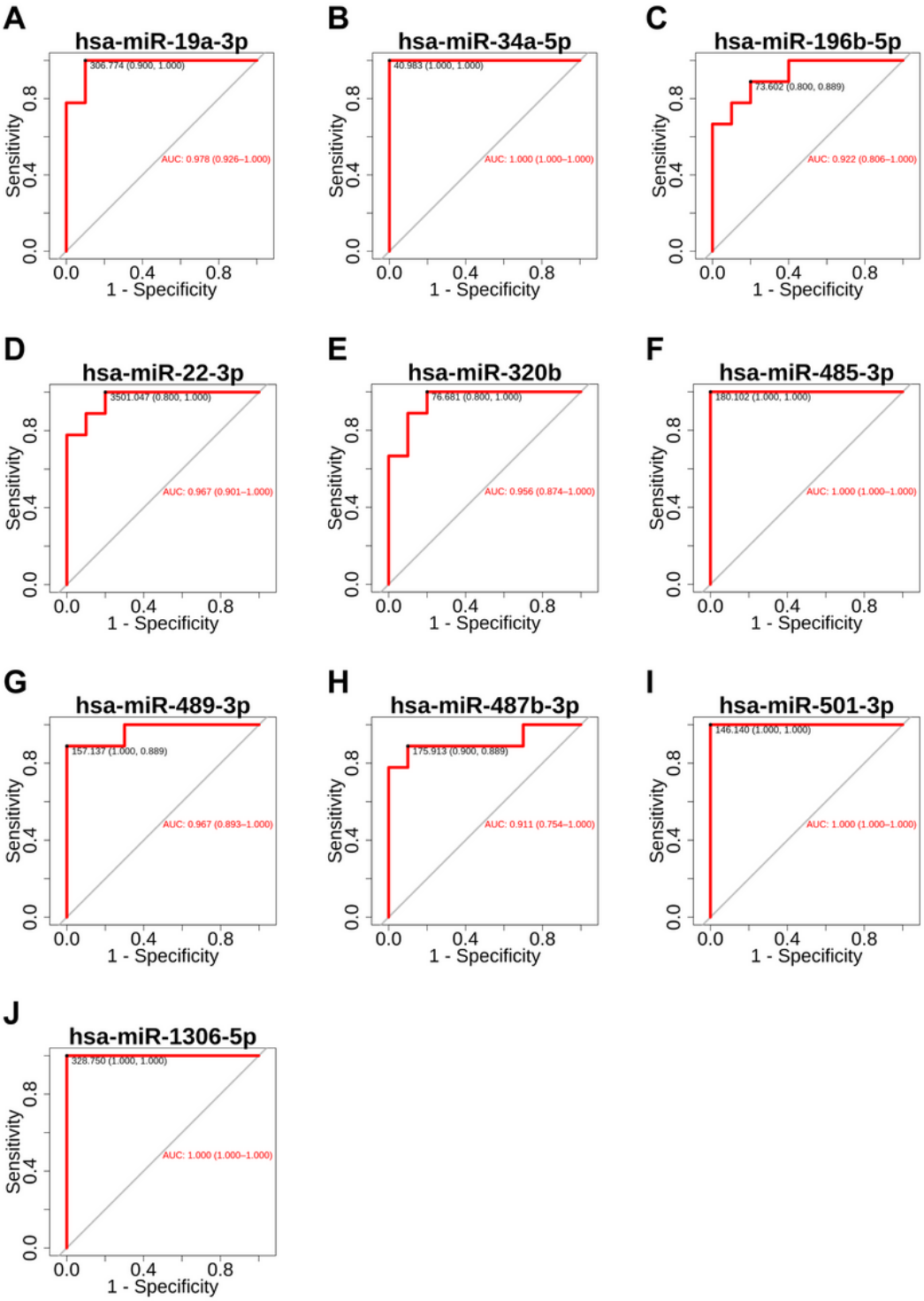

Figure 5

AUC analysis of receiver operating characteristic (ROC). The 10 miRNAs (miR-1306-5p, miR-196b-5p, miR-19a-3p, miR-22-3p, miR-320b, miR-34a-5p, miR-485-3p, miR-487b-3p, miR-489-3p, miR-501-3p) with both the sensitivity and specificity above 0.8.

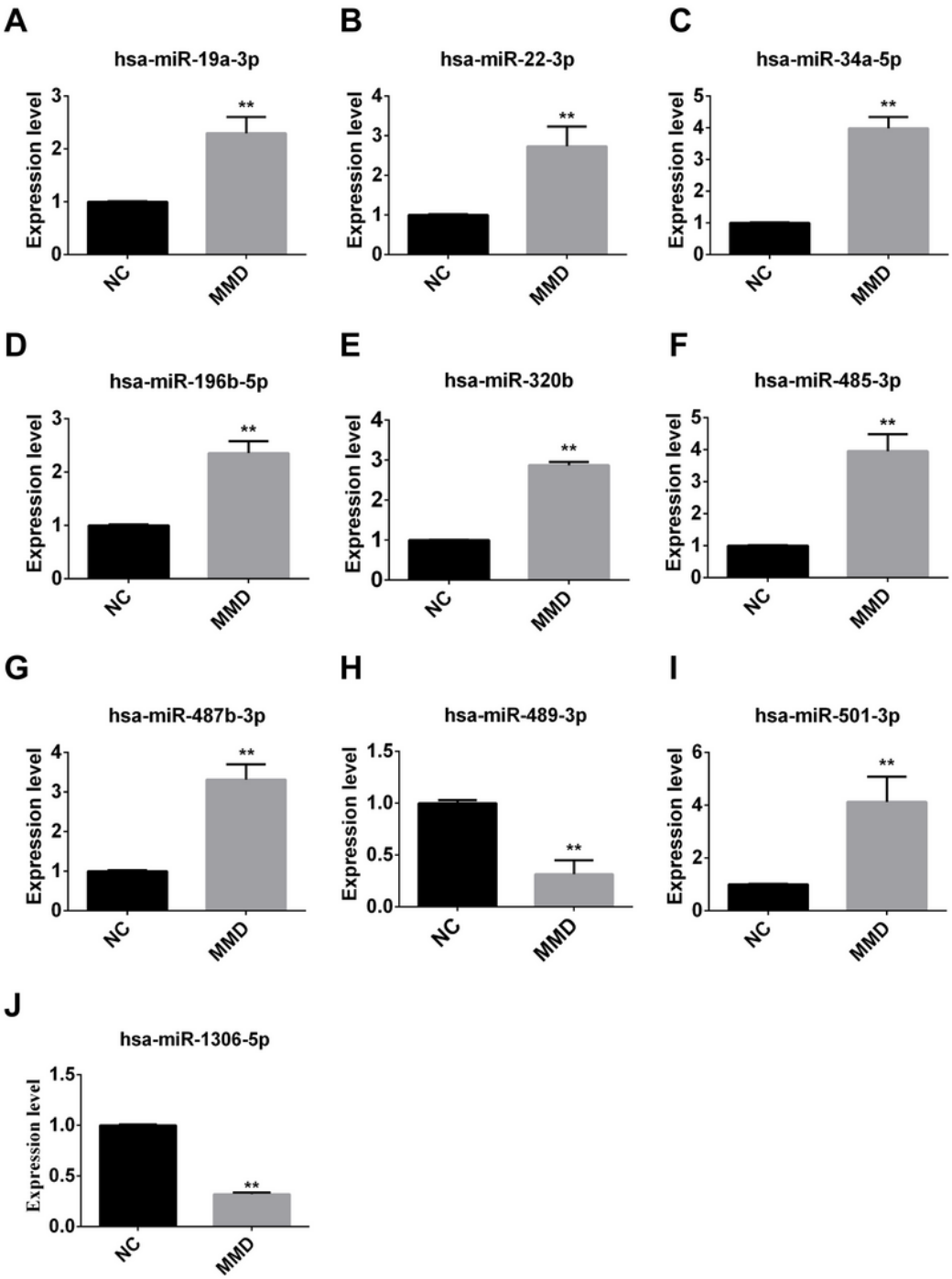

Figure 6

The levels of miRNAs were analyzed by RT-QPCR. The different expression levels of ten miRNAs (miR-1306-5p, miR-196b-5p, miR-19a-3p, miR-22-3p, miR-320b, miR-34a-5p, miR-485-3p, miR-487b-3p, miR-489-3p, miR-501-3p) between 9 moyamoya disease patients and 10 healthy individuals. NC, normal control. MMD, moyamoya disease. The data represent the mean ± S.E.M. of three independent experiments. *P<0.05, **P<0.01